Arabian Journal of Geosciences (2022) 15: 164
https://doi.org/10.1007/s12517-021-09215-4

REVIEW PAPER

Assessment of the weather research and forecasting model in simulation of rainfall for Khorasan Razavi Province, Iran

Rasoul Sarvestan[1] · Mokhtar Karami[1] · Reza Javidi Sabbaghian[2]

Received: 15 July 2021 / Accepted: 15 November 2021 / Published online: 14 January 2022

Abstract

This paper aims to assess and simulate rainfall in the cities of Khorasan Razavi Province to warn and control floods using the Weather Research and Forecasting (WRF) model. For this purpose, the two rainfall events were selected as the representative of the most severe rains that caused a lot of human and financial losses to the province. Accordingly, the five WRF model schemes, i.e., Purdue-Lin (Lin), WRF Single-Moment class 3, 5, 6 (WSM3, WSM5, WSM6) and WRF Double-Moment class 5 (WDM5), were used to perform rainfall simulation. Also, the six verification methods, i.e., threat scores (TS), false alarm ratio (FAR), hit rate (H), false alarm rate (F), Peirce skill statistic (PSS), and *R*-squared (R^2), were employed to determine the simulation accuracy. The findings showed that for the desert climates, the WDM5 scheme with R^2 of 78%; for the semi-desert climates, the Lin scheme with R^2 of 98%; for the temperate mountain climates, the WSM3 and WSM6 schemes with R^2 of 98% and 72%; and for the cold mountainous climates due to their high altitude and mountain, all schemes with R^2 of 1 were employed. The research results also showed that the TS verification method for the Lin and WDM5 schemes have more acceptable results with 66% and 63% rather than the other schemes. Also, the FAR for the Lin scheme with the lowest result (36%) is the best scheme in simulation and rainfall forecast for flood risk warnings in the province. Overall, the research results showed that foresting WRF model schemas according to the climate of each region could be suitable for flood warnings and control, and provide more time to protect people's lives and property in the next 24 h.

Keywords Flood · Climate · Rainfall · Schemes · WRF model

Introduction

Climate change has led to an increase in the frequency of natural hazards such as surface erosion and floods in recent years (Ghazali et al. 2018; McClymont et al. 2020). Forecasting these natural hazards is crucial for many programs, such as design, flood risk management (FRM), and socio-economic development on global, regional, and local scales (Kidd et al. 2017; Hu et al., 2020b). Flood forecasting is one of the most effective tools to reduce flood risk and prevent major damage (Yatheendradas et al. 2008; Papathanasiou et al. 2015; Tian et al. 2019). These available and reliable forecasts are increasingly important for understanding flood trends as well as their impacts on water resources and crisis management (Steduto et al. 2009; Xavier et al. 2016; Amorim et al. 2020). But accurate forecasting of floods strongly depends on the quality of rainfall data (Garambois et al. 2015). That is why rainfall data are one of the most important inputs used in simulations and hydrological forecasting (Kitanidis and Bras 1980; Bárdossy and Das 2008; Yonese et al. 2018; Hu, et al. 2020a, b), estimation of rainfall data is often accompanied by uncertainties related to spatial/temporal variations and the non-uniform distribution of rainfall grids. This uncertainty severely affects the information required, the warning, and the flood forecast (Bayat et al. 2019). Therefore, numerical weather prediction (NWP) systems are needed more reliably to forecast rainfall (input data in hydrological models) (Yang et al. 2015; Liu et al. 2015; Tian et al. 2017). Advances in numerical modeling make it possible to provide simulations and rain forecasts

Responsible editor: Zhihua Zhang

✉ Mokhtar Karami
M.Karami@hsu.ac.ir; M.Karami08@yahoo.co.uk

[1] Department of Climatology, Faculty of Geography and Environmental Sciences,, Hakim Sabzevari University, Sabzevar, Iran

[2] Department of Civil Engineering, Faculty of Engineering, Hakim Sabzevari University, Sabzevar, Iran

at increasingly higher resolutions in space and time (Liu et al. 2012). One of these advanced numerical models is the Weather Research and Forecasting (WRF) model, which is often used to provide rainfall estimates in regional scaling (Basin 2017; Chawla et al. 2018). This model can explicitly simulate the relationships between climate phenomena at different scales and regional rainfall with reliable accuracy (Gadgil and Sajani 1998; Ratna et al. 2011; Srinivas et al. 2013; Chawla et al. 2018). This model also recognizes a large part of floods (before they occur) each year by reliably simulating rainfall, and prevents socio-economic damage before it occurs (Evans et al. 2000; Cong et al. 2006; Casagli et al. 2006; Chen and Hossain 2018).

Tahir et al. (2017) used a multilayer neural network model to quantitative precipitation forecast (QPF) and apply their numerical output in hydrodynamic models to predict floods in a tropical region in northeastern Peninsular Malaysia. The results showed that this model can predict rainfall for the next 1 h with acceptable accuracy and can be used for a larger area.

Minamiguchi et al. (2018) assessed the performance of the WRF for simulating a series of August 2014 rainfall events over Japan and investigated the impact of uncertainty in sea surface temperature (SST) on simulated rainfall in the record-high precipitation period. Murthy, Saravana, and Kumar (2018) predicted rainfall in Northeast India using the Seasonal Autoregressive Integrated Moving Average (quite a mouthful) (SARIMA) model. They showed that the SARIMA (0,1,1)(1,0,1) model is suitable for analyzing future rainfall patterns. Ridwan et al. (2020) predicted rainfall using four machine learning methods in the Terengganu region of Malaysia. They indicated coefficients between 0.5 and 0.9 with the highest of each scenario for daily, weekly, 10-day, and monthly rainfall. In method 2 (M2), the overall model performance shows that normalization using a log-normal distribution is preferably giving a good result for each category except for 10 days with the Boosted Decision Tree Regression (BDTR) and Decision Forest Regression (DFR) giving the most acceptable result than Neural Network Regression (NNR) and Bayesian Linear Regression (BLR). So, two different methods were applied with different scenarios for different time horizons. Method 1 (M1) illustrates a relatively higher accuracy than M2 using BDTR modeling. This accurate rainfall forecasting is crucial. Besides, the improvement of flood warnings can prevent loss of life and property damage due to flash floods associated with rainfall (Hasan and Islam 2018).

In Khorasan Razavi Province, the placement in arid and semi-arid regions of the country every year during the spring and summer seasons, heavy rains, showers, and floods causes extensive human and financial damage to urban areas. Accordingly, in this research, to this warning of the danger of floods, measures and solutions must be taken to protect people's lives. One of the most important measures and solutions is to reduce flood damage, use the forecasting of the meteorological WRF model, and use the numerical output of this model in hydrological models at the urban level. For this purpose, for the accuracy of this model in simulating and forecasting rainfall in different climates of the province, two of the most severe rains that caused flood damage and damage to urban areas in the province were selected. The most important questions considered in this study are as follows: (i) What is the accuracy of the meteorological WRF model in simulating rainfall in different schemas for each of the climates? (ii) What are the types of different schemes in different climates? (iii) Is the output of the WRF model accurate enough to be used to predict rainfall in the next 24 h?

Methods and data

Study area

Khorasan Razavi Province is located in the northeastern of Iran, between 56° and 19′ to 61° and 16′ east longitude and 33° and 52′ to 37° and 42′ north latitude. It extends to Turkmenistan northerly, to Afghanistan easterly, to North Khorasan, Semnan, and Yazd provinces northerly and westerly, and to South Khorasan and Yazd provinces southerly and southwesterly (Statistical yearbook 2019) (Fig. 1).

One of the characteristics of rainfall in is rainfall occurring in the cold season (starting from autumn to spring) with an abnormal distribution. Short-term torrential and rain showers are a significant part of annual rainfall. The average rainfall of the province during the period 1989–2018 is 209.5 mm. This is while the average rainfall in Iran is 232.4 mm, and the global average rainfall is 780 mm. It is observed that the rainfall of Khorasan Razavi Province is about a quarter of the global average rainfall, so it is one of the least rainy regions in the world. The distribution of rainfall in the province is not uniform: its amount decreases from north to south. The findings also showed that the lowest average annual rainfall in Khorasan Razavi in Bardaskan City was 114.6 mm, and the highest amount in Ghouchan was 310.2 mm (Fig. 2a).

Khorasan Razavi Province has hot summers and relatively cold winters. The average annual temperature increases from north to south. The average yearly temperature of Fariman City, as the coldest region of Khorasan Razavi, is 4.12 °C. The study of the average annual temperature also showed that Bardaskan City with 19.8 °C (Fig. 2b) has the highest temperature in the province (Iran Meteorological Office, 2019).)

Observation data

Observational data for two 12 April 2020 and 24 May 2020 rainfall events were extracted from 11 synoptic

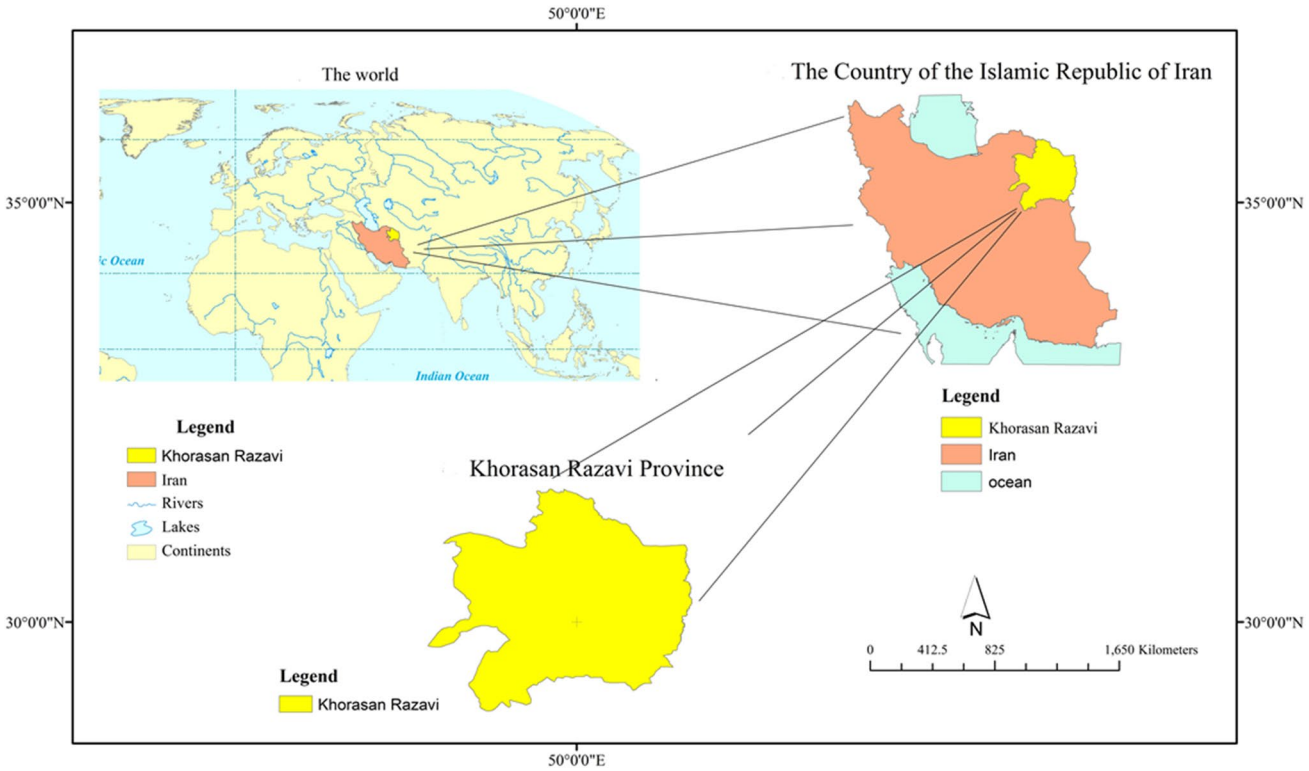

Fig. 1 Geographical map of the study area

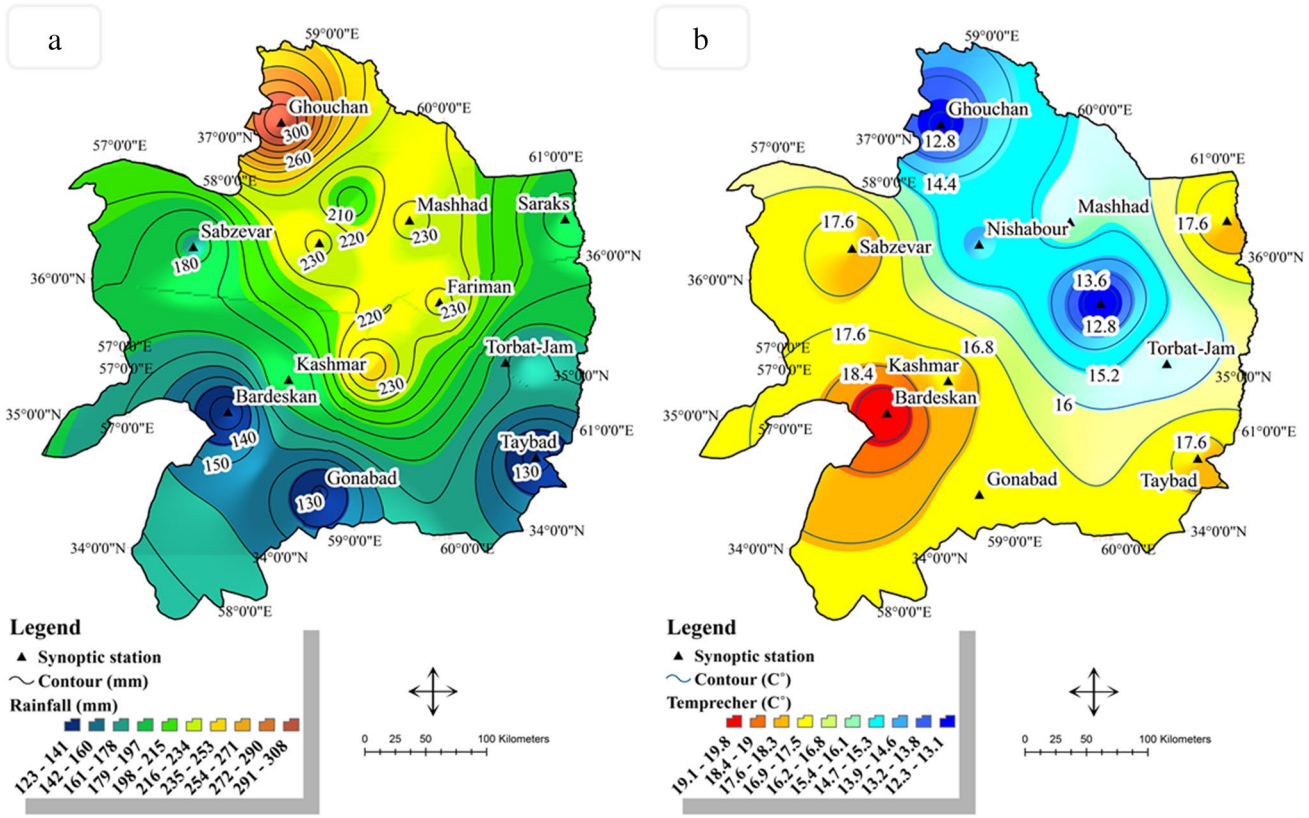

Fig. 2 **a** Map of the average annual rainfall. **b** Average annual temperature in Khorasan Razavi Province

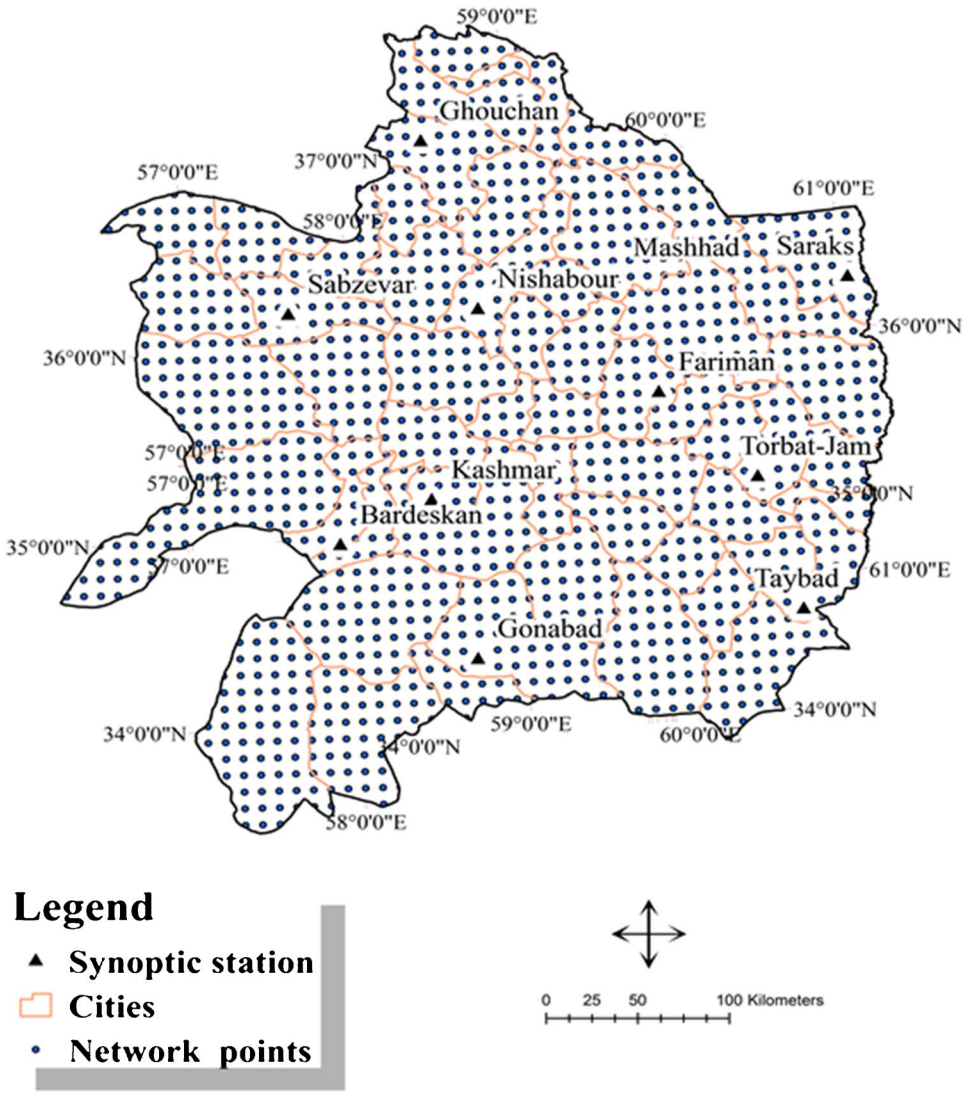

Fig. 3 Synoptic station (black). Map network points resulting from the output of the WRF model (blue)

Table 1 Specifications of stations and observational data

Rows	Stations	Longitude	Latitude	Altitude	Events (mm)	
					24 May 2020	12 April 2020
1	Torbat_jam	60˚35′	35˚15′	950	13.3	8
2	Sabzevar	57˚43′	36˚12′	972	36	28
3	Saraks	61˚10′	31˚12′	280	27.2	11
4	Ghouchan	58˚30′	37˚40′	1287	9	18.5
5	Kashmar	58˚28′	35˚12′	1110	34.2	11
6	Gonabad	58˚41′	34˚21′	1056	13.3	0.1
7	Mashhad	36˚16′	59˚38′	999	49.8	8
8	Neyshabour	58˚48′	36˚16′	1213	22.2	20.1
9	Fariman	59˚50′	35˚30′	1400	17.3	16.2
10	Taybad	60˚47′	34 ˚44′	900	7.9	7
11	Bardeskan	57˚57′	35˚16′	1011	9.3	5.1

stations in Khorasan Razavi Province associated with Iran Meteorological Office. Since the present study is related to the simulation of rainfall quantity, for better analysis of the year's rainy seasons (spring and summer)

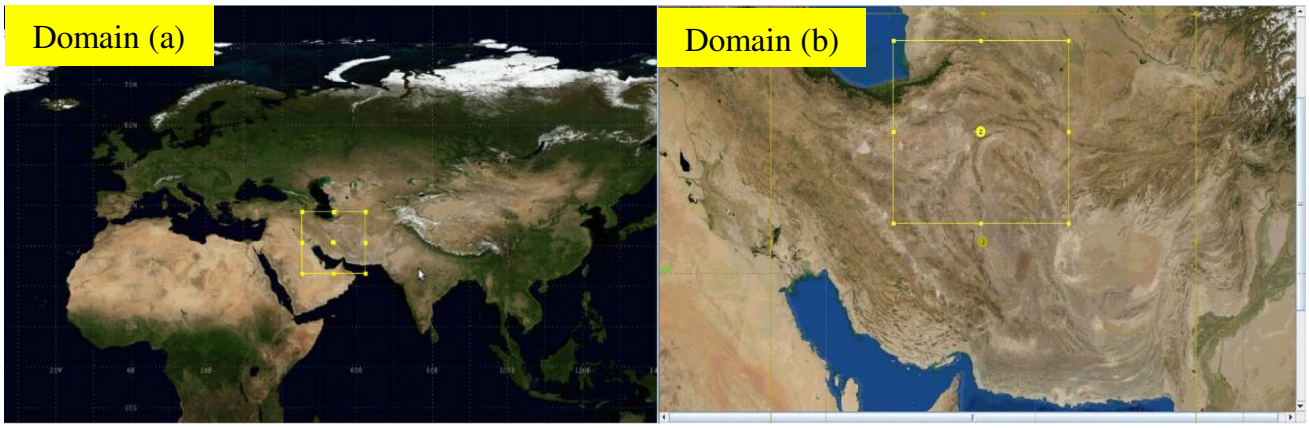

Fig. 4 The outer and internal domains of the WRF model. **a** The outer domain of the model with a spatial resolution of 15 km. **b** The inner domain of the model with a spatial resolution of 5

were examined. Figure 3a and b and Table 1 show the distribution of available stations. The 12 April 2020 and 24 May 2020 rainfall events were two of the most severe events. The 12 April 2020 rainfall event in Khorasan Razavi was affected by a severe storm that caused widespread flooding and destroyed most villages. The event on 24 May 2020 in the whole province caused floods, causing many human and financial losses to urban, rural, and agricultural areas. At most stations, precipitation data are reported cumulatively for 6 h at 00, 06, 12, and 18 UTC. In some cases, cumulative rainfall is reported for 18 h at 06 UTC and 6 h at 12 UTC. But what is needed in this research is 24-h cumulative rainfall, so considering that the model was run for 24 UTC, these rains must have occurred from 06 to 06 UTC.

Ensemble prediction systems (EPS)

These systems are presented to estimate the uncertainty of the initial condition in weather forecasting and simulation. Various meteorological services and centers including European Centre for Medium-Range Weather Forecasts (ECMWF), National Centers for Environmental Prediction (NCEP), Japan Meteorological Agency (JMA), United Kingdom Meteorological Office (UKMO), Meteorological Service of Canada (MSC), Global Forecast System (GFS), and other similar centers provide homogeneity of precipitation by solving numerical equations of weather across the globe (Hsiao et al. 2013; Goodarzi et al. 2018). It should be noted that the forecasts of these centers are networked on a large scale. In this research, Ensemble GFS prediction system is used to simulate study events. After selecting the ensemble system, the WRF model has been used for the dynamic downscaling of the study area. Then five different configurations are considered for the selected model. Two domains have been used for this research.

(a) Spatial coverage covers 15 km and ranges from 24 to 42° north and 42 to 66° east (on Iran) (Fig. 4a).
(b) Spatial separation covers 5 km in the range of 31–42° north and 53–63° east (on Khorasan Razavi) (Fig. 4b).

The model is run daily for 06 UTC hours and is produced in each run for the next 24 h. The horizontal separation of roughness and land use data was 2 min (about 4 km). For the boundary and initial conditions, the GFS[1] data was used since the output of the WRF model is without format.

WRF Model

The Weather Research and Forecasting (WRF) model is a next-generation mesoscale numerical weather prediction system designed for atmospheric research and operational simulating applications. It features two dynamical cores, a data assimilation system, and a software architecture supporting parallel computation and system extensibility. The model serves a wide range of meteorological applications across scales from tens of meters to thousands of kilometers (https://www.mmm.ucar.edu/weather-research-and-forecasting-model).

In this simulation, the WRF version[2] 4.1.5 was employed. The WRF is a state-of-the-science medium-scale meteorological model. It makes simulations based on actual atmospheric conditions or idealized conditions feasible (Zhang et al. 2021; Langkamp and Böhner 2011). The equations set for the WRF are fully compressible and Eulerian

[1] .https://www.ftp.ncep.noaa.gov/data/nccf/com/gfs/prod/
[2] . https://github.com/wrf-model/WRF/releases

Table 2 Features of configuring and executing the WRF model

Configuration	Outer domain	Inner domain
WRF version	WRF 4.1.5	
Grid spacing (km)	15 km	5 km
Horizontal grids	100 × 132	88 × 100
Vertical grids	42 layer/top 50 hPa	
Integration time (s)	90	60
Radiation	Dudhia shortwave	
Surface layer	5-layer slab, single-layer, UCM, Monin–Obukhov	
Cumulus	Kain-Fritsch	
Planetary boundary layer	SH	
Microphysics	Lin, WDM5,WSM3,WSM5,WSM6,	
Initial boundary condition	Global Forecasting System (GFS) model simulate fields (27-km resolution)	

non-hydrostatic with a run-time hydrostatic option. It is conservative for scalar variables. The prognostic variables consist of velocity components u and v in Cartesian coordinates, vertical velocity w, perturbation potential temperature, perturbation geopotential, and perturbation surface pressure of arid air, as well as several optional prognostic variables depending on the model physical options (Zhang et al. 2021; Skamarock et al. 2005, 2008; Wong et al. 2012). In this paper, five microphysics including WSM3, WSM5, WSM6 (Hong and Lim 2006; Hong et al. 2004; Naing 2021), WDM5 (Hong et al., 2010; Wang et al. 2011; Guo et al. 2019; Mahala et al. 2021), and Lin (Cao et al. 2021) were employed to assess rainfall simulation with observational values in study stations. Each of these schemes performs microphysical schemes on the study area. Then, according to the climatic representative, it is determined with which of these climatic representatives each of these schematic representatives correctly predicts the amount of rainfall (Table 2).

Simulate verification

The simulate verification method is the assessment of the quality of meteorological simulate data. The simulate results are compared with observational data to ensure the results of simulate data for the future. There are different methods for predicting that can be verified, but in this study two methods are used (Mohammadiha et al. 2012).

Two-state simulate agreement table (2 × 2)

One of the standard methods for examining the model's performance in predicting its rainfall is considered a binary corpus. For each of the different precipitation thresholds, a 2 × 2 agreement table is formed, and then the numerical quantities corresponding to each table are calculated. Finally, the conclusion is based on the analysis of these committees.

Assuming that O and Y, respectively, represent the observations and simulants, Table 3 is formed as follows, the variables of which are:

O1 Positive observations (occurrence of the phenomenon)
O2 Negative observations (absence of phenomenon)
Y1 Positive simulants (occurrence of the phenomenon)
Y2 Negative simulants (absence of phenomenon)
a The number of times the phenomenon has occurred and its occurrence has been simulated
b The number of times the phenomenon has not occurred, but its occurrence has been simulated
c The number of times the phenomenon has occurred, but its occurrence has not been simulated
d The number of times the phenomenon has not occurred, but its occurrence has not been simulated

Fence quantities dependent on the agreement Table 2 × 2

Although the 2 × 2 agreement table specifies the simplest type of simulation, accurate measurement of this type of simulation with this table requires at least three numerical quantities (equal to the dimension of the problem). In other words, the additional function of simulate lies in this table,

Table 3 Dependent to the agreement Table 2 × 2

	O1	O2	
Y1	a	b	$a+b$
Y2	c	d	$c+d$
	$a+c$	$b+d$	$N=a+b+c+d$

Table 4 Statistical metrics applied in the verification

Evaluation method	Formula	Range	Perfect value
Threat score (TS)	$TS = \frac{a}{a+b+c}$	0 ~ 1	1
False alarm ratio (FAR)	$FAR = \frac{b}{a+b}$	0 ~ 1	0
Hit rate (H)	$H = POD = \frac{a}{a+c}$	0 ~ ∞	1
False alarm rate (F)	$F = \frac{b}{b+d}$	0 ~ ∞	0
Peirce skill statistic (PSS)	$PSS = TSS = \frac{ad-bc}{(a+c)(b+d)} = H - F$	0 ~ ∞	1

i.e., it cannot be fully simulated with just one number. Different fencing committees are presented, of which only three are used below for verification.

Threat score (TS)

The TS value is equal to the ratio of the number of cases, in which the phenomenon was correctly simulated, to the total number of cases in which the phenomenon occurred or was simulated (Table 4). Its value is similar to the correct ratio, always between 0 for the worst and 1 for the best. This quantity is identical to the correct ratio, except that the cases where the phenomenon did not occur and was not simulated (d) are not considered.

False alarm ratio (FAR)

This quantity is by definition the ratio of the number of incorrect simulants to the total number of occurrences. So the smaller the value, the better it becomes 0 for the best and 1 for the worst (Kodamana and Fletcher 2021).

Hit rate (H)

It is calculated as the ratio of the number of correct simulants of a phenomenon's occurrence to the total number of observations of the phenomenon. This model is also termed Possibility of Detection (POD).

False alarm rate (F)

By definition, the ratio of the total number of incorrect simulants (unfulfilled simulants) to the total number of observations that the phenomenon has not occurred.

Table 5 Evaluation of climate classification criteria at local and global levels

Climatic classification	Type climate	A	B	C
Climate coefficients	Transeau	O	U	U
	Ivanov	O	U	U
	De Martonne	O	O	O
	Barat	O	U	U
	Koppen	O	U	U
	Seyaninov	O	U	U
Charts climate	Thornthwaite	O	U	U
	Climagraph	O	U	U
	Embrothermic	O	U	U
	Emberger	O	O	O

O, suitability of criteria in climatic classification; *U*, unsuitability of criteria in climatic classification

A Availability of basic meteorological information (because without this information it is very difficult to compare it with other methods of climatic classification)

B Importance and validity of climatic indexes (no defects in climatic coefficients of the region)

C These methods should consider at least 5 climatic classes of Khorasan Razavi Province (climatic regions of the province include desert, semi-desert, Caspian, Mediterranean, and mountainous climates)

Peirce skill statistic (PSS)

The value of this score becomes 1 for a complete simulation because b and c are equal to 0; and therefore, the values of H and F will be 1 and 0, respectively (Table 4). For worse simulants than before, the PSS value is negative, and constant simulants (always y1 or y2) are 0. For rare phenomena, the value of d is larger, and consequently, F is smaller, and TSS is closer to POD (H) (Mohammadiha et al. 2012).

Results and discussion

Climatic classification

This research needs a local climatic classification to select each of the different schemes of the WRF model in Khorasan Razavi Province. For this purpose, first, 12 global and local classification methods (Table 5) were compared to select the best climate classification. Then, a, b, and c criteria were used to measure the climates in the region.

According to these criteria, the climates of the valid De Martonne and Emberger indexes, which are more relevant today, were selected and compared in the following, since

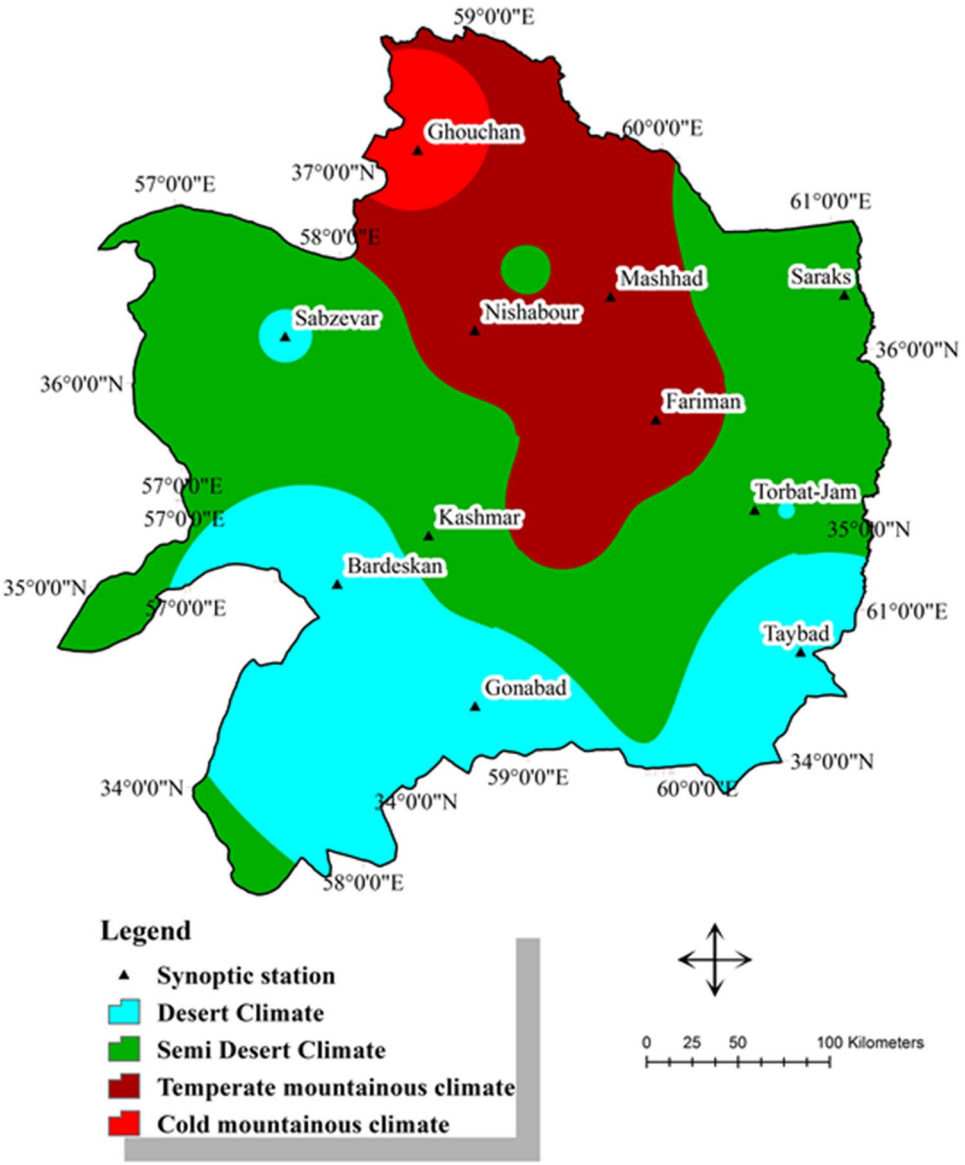

Fig. 5 Climate classification map in Khorasan Razavi Province

the number of meteorological stations and statistical period used in determining the climate of the region is effective.

And by changing the number of stations or the statistical period, the climate of the region changes. For this reason, the Emberger and De Martonne methods were generalized to the Iranian climate map (Fig. 5).

The results of this figure showed that Khorasan Razavi Province has four different types of climates according to the method of climatic regions of Iran.

Semi-desert climate has the most level of classification with four stations and cold mountain climate with one station is the lowest level of this climatic classification.

Based on the results, the mentioned method is about 70 to 75% of the province in the desert and semi-desert climates. These results choose the right evaluation criteria (a, b, and c) for a local climate and it is compatible with the results of Kamyabi (2016).

Microphysical Schemes

After determining the climate of the region, then forming 5 schemas Lin, WDM5, WSM3, WSM5, and WSM6, the WRF model was performed to simulate events in the province. By comparing these schemas, it is determined which of these local climates is related and compatible.

Figure 6a and b show the rainfall simulation status in each of the schemas for the 24 May 2020 event; the study of the findings of this figure shows that the microphysical Lin scheme has the least rainfall difference with the observation period, as it is clear this scheme has better communication and certainty in simulating rainfall in semi-desert climates than in other climates.

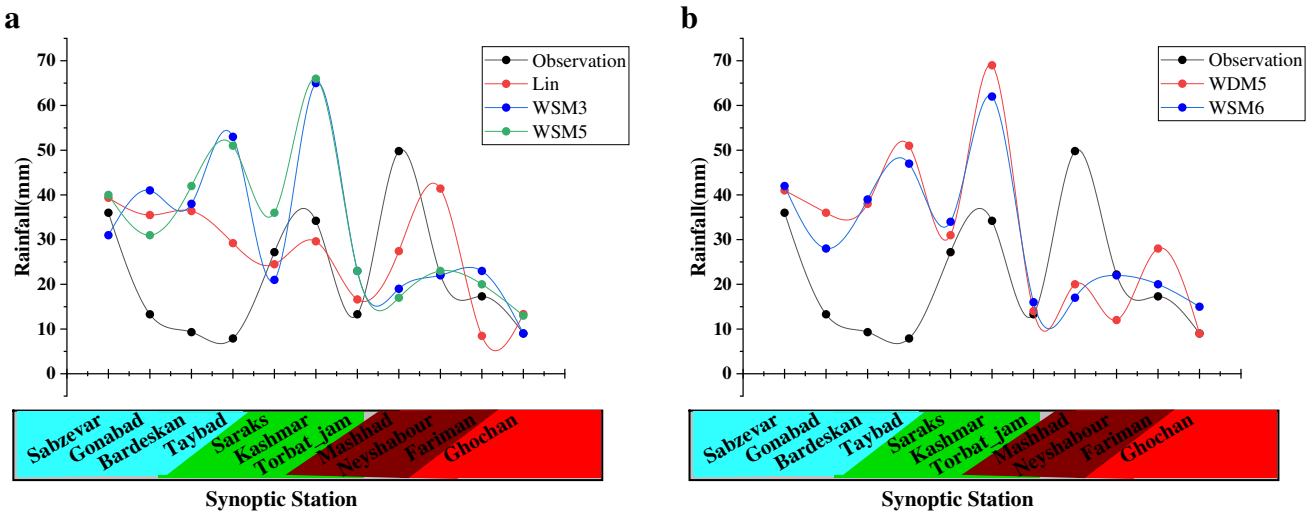

Fig. 6 Comparison of different schemes in Khorasan Razavi Province (the event on 24 May 2020)

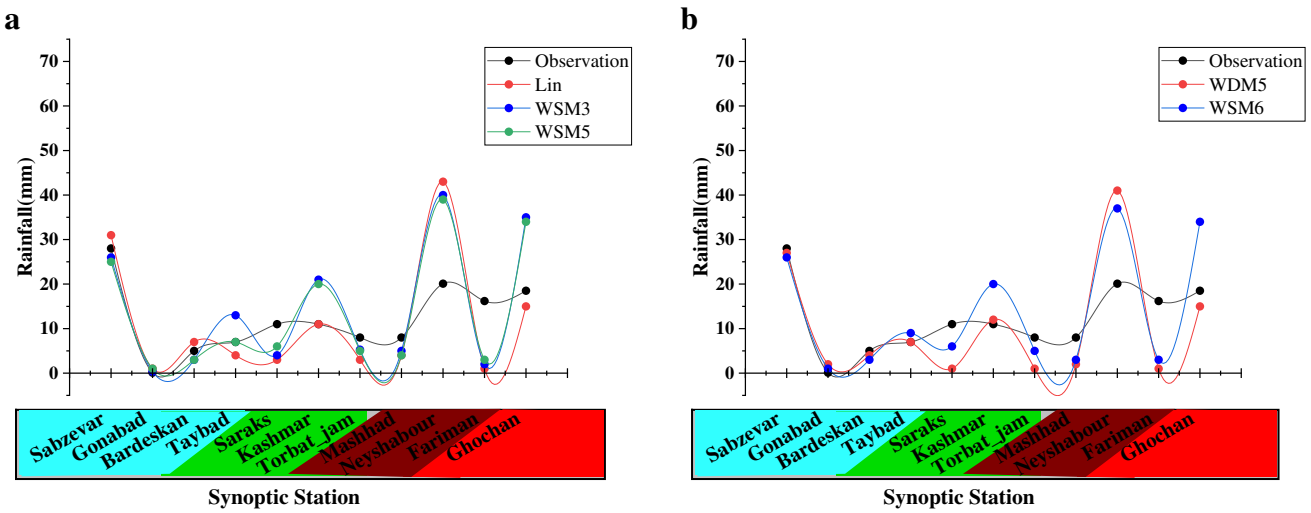

Fig. 7 Comparison of different schemes in Khorasan Razavi Province (the event on April 12, 2020)

The stations of this climate are Torbat-Jam, Sarakhs, and Kashmar where the amount of rainfall difference with the observation period was simulated − 0.37, 2.41, and − 2.70 mm in 24 h, respectively.

This scheme can better simulate rainfall in semi-desert areas due to the combination of six categories of water vapor materials, including water vapor, snow, ice, rain, cloud water, and snowflakes. These results are consistent with the results of Hadilooie et al. (2014).

After the semi-desert climate, the cold mountain climate in this schema also has very good results with observational values. As is known, in this climate, the Ghouchan station simulated rainfall with a difference of 0.41 mm.

Figure 7a and b show the amount of simulated and observed rainfall for the 12 April 2020 event. The simulation of this event shows that WDM5 and Lin schemes have the least differences in observational values in desert climate schema, respectively. In the desert climate, the stations Taybad with 0 mm, Bardaskan with − 1 mm, Sabzevar with − 1 mm, and Gonabad with 1.9 mm differ with observational values. The WDM5 schema assessment is good for desert climates because it has two parameters for hot water processes and five microphysical categories of ice, cloud, and rain density. The WDM5 scheme was performed better in rainfall simulation for the desert climate and it is consistent with the results of Kakolaki et al. (2016). In the study of two schemes, as WSM3 and WSM6 show, these schemas simulate rainfall more than observational values. Therefore, these two schemas are not suitable for the province's climate. These are mostly used for the humid and Mediterranean

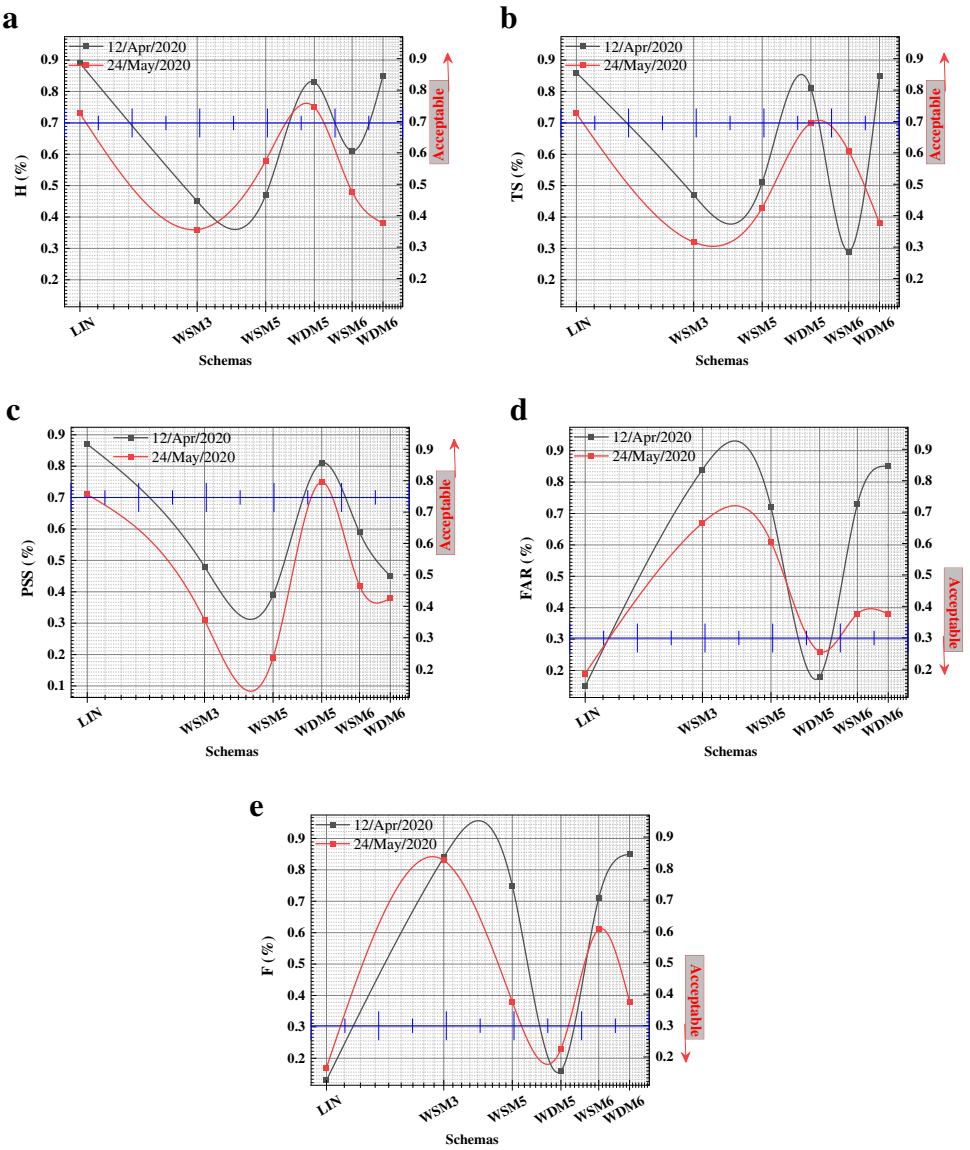

Fig. 8 Assessment of the various schemas in studies of the events

climates, and this result is consistent with the results of Que et al. (2016)

Simulate verification model

Assessment of different schemes of the WRF model for two events shows 24 May 2020 and 12 April 2020. In both events, the Lin and WDM5 schemas perform best according to the verification criteria.

Assessment of the positivist verification criteria, PSS, TS, and H, shows that these values are higher at above 70% and close to 1. The accuracy of the schemas in simulating the rainfall of events is more acceptable (indicated by the up arrow). Thus the lower the values of these criteria than 70% and close to 0, the weaker the scheme assessment in rainfall simulation (Fig. 8a, b and c). Also, the assessment of the negative verification criteria, F and FAR, shows that the lower these values are, the closer they are to 30% and close to 0. The accuracy of the schemas in simulating rainfall is more acceptable (indicated by the down arrow). And the higher the values of these criteria than 30% and close to 1, the weaker the schema assessment in rainfall simulation (Fig. 8d and e) Mohammadiha et al. (2012). From the verification criteria of positivism and negativism, it was determined that the *H* criterion in the positivity criterion and the *F* criterion in the negativity criterion assess rainfall with a more acceptable simulation.

Figure 9a, b, and c show the assessment of the acceptability (arrow mark) of each of the schemas in climates and stations. Examination of the findings of these figures shows that the Lin scheme works better in the semi-desert climate.

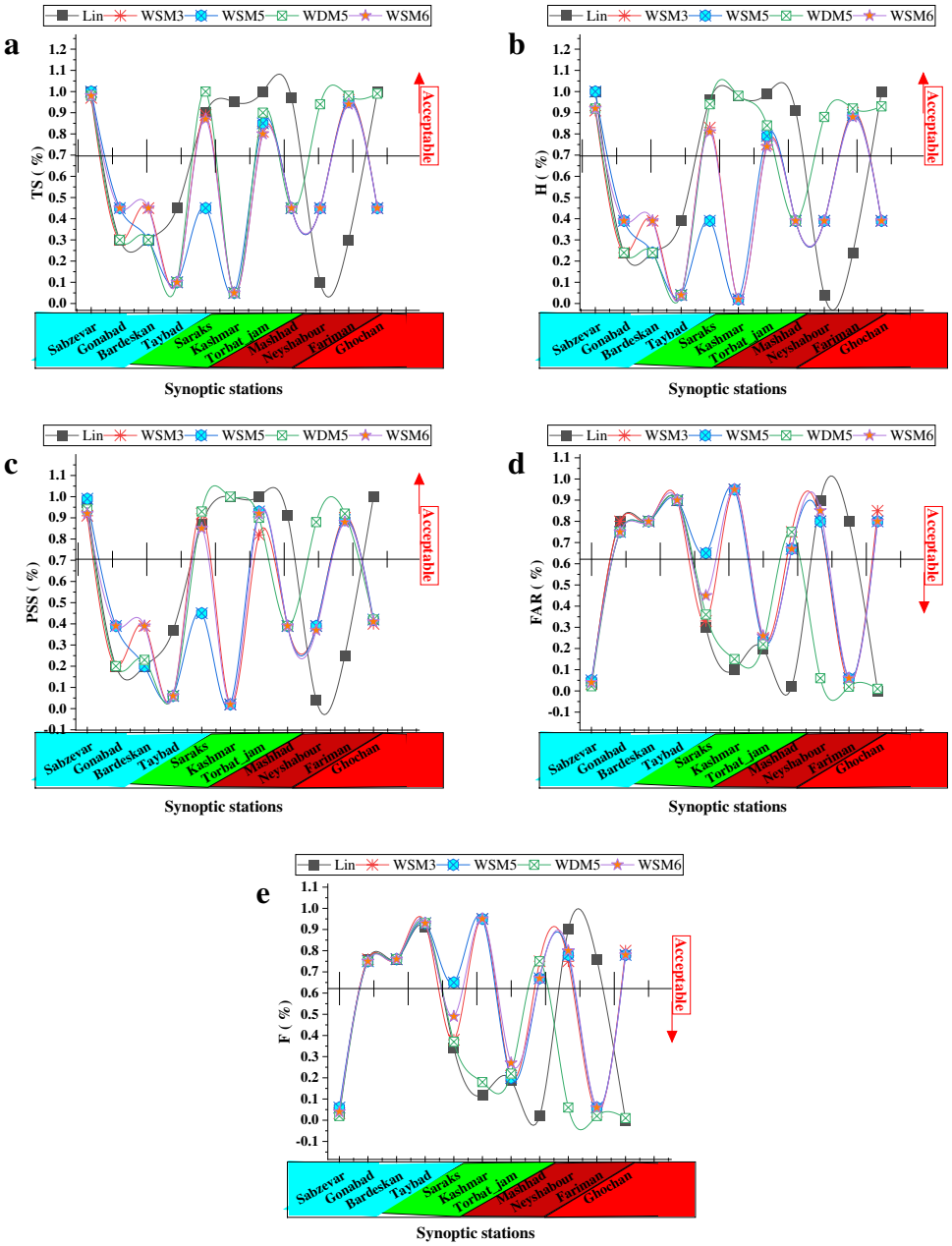

Fig. 9 Simulate rainfall of the schemes in the various climates

In these climates, the values of hit rate (*H*), threat score (TS), and Peirce skill statistic (PSS) were 97%, 96%, and 95%, respectively. This schema can actually simulate rainfall in a semi-desert climate with acceptable accuracy. This climate also has a good performance in simulation on stations of other climates such as Sabzevar in desert climate, Mashhad in temperate mountainous climate, and Ghouchan in mountainous climate.

Figure 9d shows the false alarm ratio (FAR) to the number of simulations performed in a 24-h simulation. Due to the relationship between tables, this quantity has a negative tendency. In other words, its lower values indicate more simulation skills. As shown in Fig. 9, the Lin scheme in semi-desert climates is better related and more compatible than other schemes. In this climate, the average quantity of FAR is 0.2.

In Fig. 9e, the number of false alarms (*F*) is the ratio of the total number of false simulations to the total number of observations that the phenomenon did not occur. So this quantity is negative; that is, the lower the quantity, and so the accuracy of the model, and the schemes' results will be more acceptable. As can be seen from the results, the Lin and WDM5 schemes have lower values which are 21% and 25%, respectively.

Table 6 Coefficient R^2 for each of the different climatic schemas (the event on May 24, 2020)

Group	Climate	Lin	WSM3	WSM5	WSM6	WDM5
1	Desert	0.73	0.33	0.06	0.006	0.63
2	Semi-desert	0.98	0.31	0.47	0.42	0.52
3	Temperate mountain	0. 50	0.98	0.62	0.72	0.01
4	Cold mountain	1	1	1	1	1

Table 7 Coefficient R^2 for each of the different climatic schemas (the event on April 12, 2020)

Group	Climate	Lin	WSM3	WSM5	WSM6	WDM5
1	Desert	0.78	0.52	0.06	0.01	0.65
2	Semi-desert	0.84	0.01	0.00	0.41	0.75
3	Temperate mountain	0.36	0.35	0.40	0.42	0.40
4	Cold mountain	1	1	1	1	1

To better assess each of the various schemas in the climates, a coefficient of R^2 was used between the observation and simulation data for the two events. Table 6 shows the assessment status of each of the schemas in various

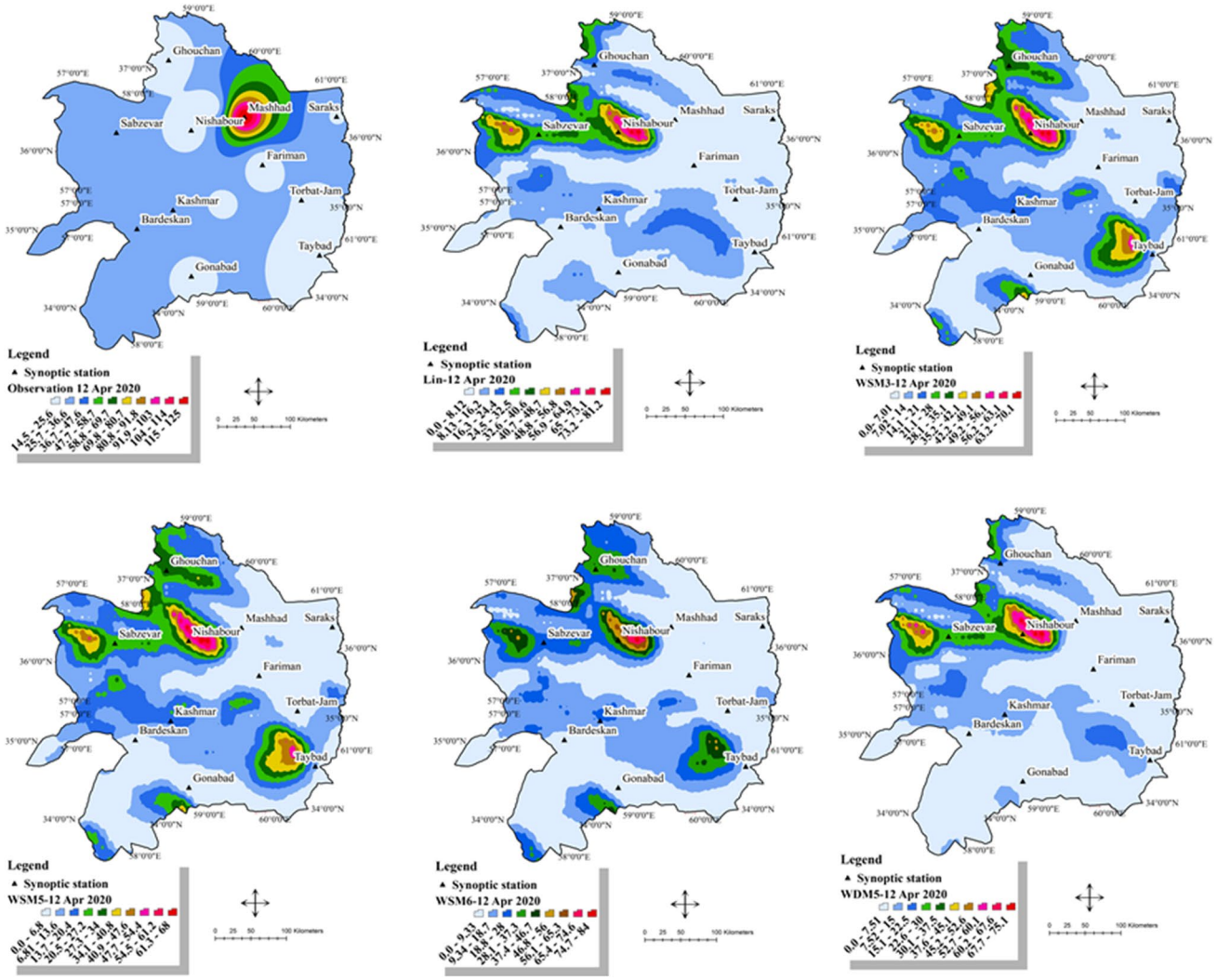

Fig. 10 Observed and simulated rainfall in different schemes for the event on 12 April 2020

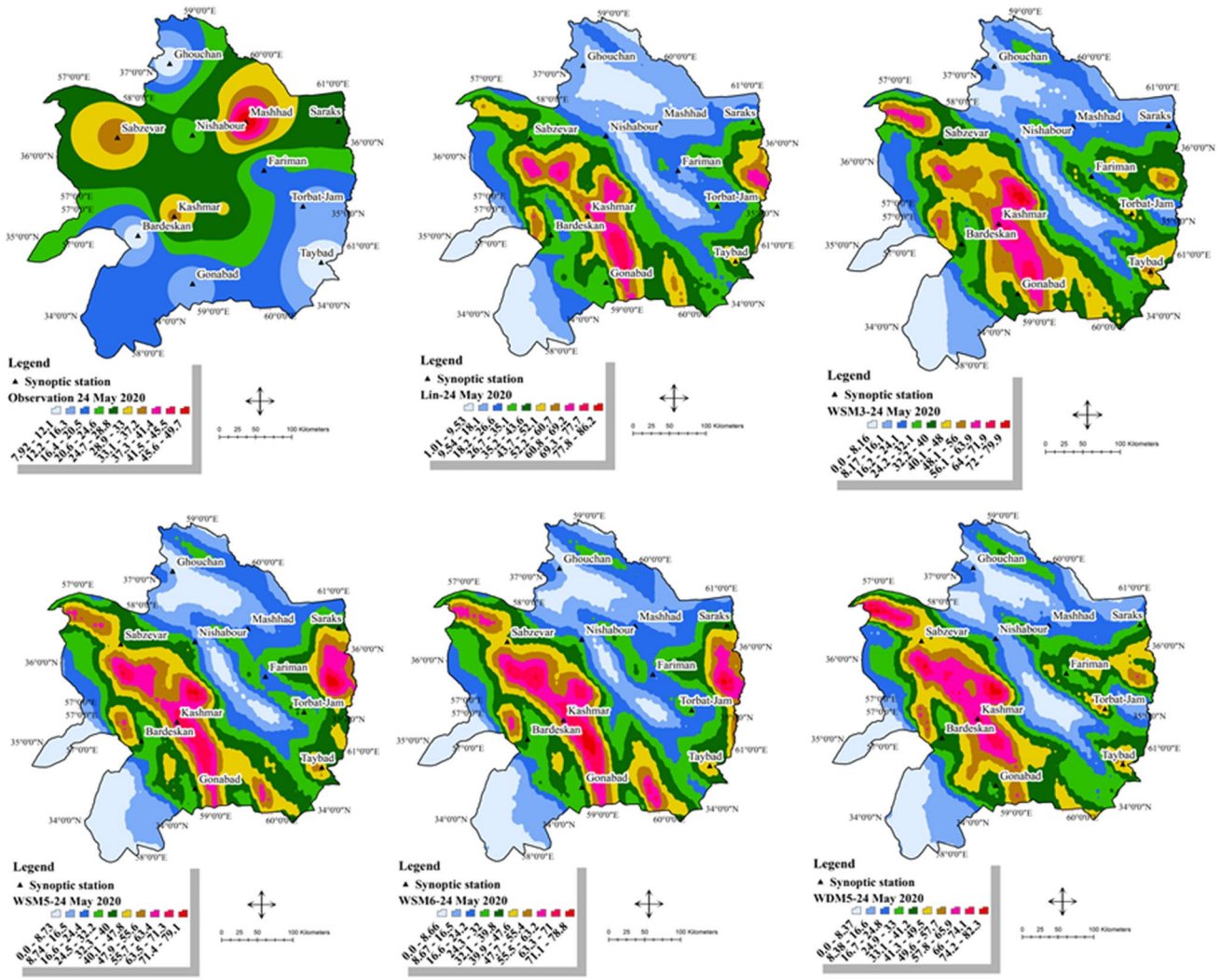

Fig. 11 Observed and simulated rainfall in different schemes for the event on 24 May 2020

climates for the 24 May 2020 event. As is known, the Lin schema has the highest value of R^2 coefficients in cold mountainous climates with 1%, semi-desert with 98%, and desert with 73%. This indicates that the Lin schema has a more acceptable assessment in simulating rainfall in various climates. The cold mountainous climate has more acceptable results between the amounts of simulations of observation data due to its high altitude and mountainous nature. In this respect, it is consistent with the research of Mohammadiha et al. (2012).

Table 7 shows the coefficient R^2 observation rainfall results with the simulation data for the April 12 event in the climatic various conditions. In this event, Lin and WDM5 schemes have the highest R^2 coefficient in simulating rainfall over various climates.

The value of R^2 in the Lin schema is from highest to lowest accuracy, respectively, in cold mountainous climates with 1, semi-desert with 84%, and in desert climates with 78%.

Figures 10 and 11 show rainfall simulation maps in various designs for study events. In these maps, due to the small number of synoptic stations compared to the WRF model simulation points, the simulation values are different in non-station areas. (Since hydrological models in various points of the earth surface present deficient data and this causes bias and error in simulation estimates in various points, therefore, one of the main objectives of this study is to use the output of the WRF model for points without stations. This output is used in 9-km networks and also at a distance of 5 km from the synoptic station, for input in hydrological models.) Analyzing these figures shows that various schemes should be used for each climate of the province. For example, in semi-desert climates, Kashmar, Torbat-Jam, and Sarakhs stations, and, in the cold mountainous climate, Ghouchan station have an acceptable accuracy in simulating

rainfall with observation amount. This accuracy differs in the weather areas and stations of the province. For example, it simulates the amount of rainfall in some areas, such as cold mountain climates and semi-desert climates, with acceptable accuracy.

The findings also showed that the most suitable climates according to the meteorological model schemas for temperate mountainous climate Lin and WDM5 schemes have the best rainfall simulation compared to other climates.

According to the research findings, it was determined that the WRF meteorological model has an acceptable power in simulating rainfall on the climates of the study area. Although the amount of rainfall simulated in different schemes is different and some simulate more and less than the actual value, in fact this model is able to simulate the amount of rainfall in selected schemas with the least possible difference.

A comparison of this study with previous research showed that the WRF model is more accurate than other methods and models used: for example, compared to radars and satellites in research such as Shahrban et al. (2011), Gerber et al. (2018), and Li, Chen, and Lin (2021), and compared to numerical models with research (Kusaka et al. 2005; Zhu et al. 2021; Li, Chen, and Lin 2021; Bhimala and Gouda 2021) that simulates rainfall with higher accuracy and assessment.

The strength of this research is that most of the previous researches of Bhimala and Gouda (2021) have been done on simulation and forecasting of precipitations without considering the use of their numerical quantity in urban and river basins. However, if in this study, by selecting the selected schemas by simulating rainfall in each climate, they are simulated in the next 24 h, then the numerical output of this meteorological model is used in hydrological models in the city. And another strength of this method became known before the occurrence of floods and flood events in urban areas. This can prevent flood damage in different places.

Conclusions

Since floods are natural disasters that cause human and financial losses, communities need to manage and implement strategies to reduce the damage. One of these solutions is flood forecasting and warning systems, which are used as one of the most important flood management. Confidence in these systems is checked in all countries of the world. For this purpose, these systems must be examined and verified to be exploited and used in the study area. One of the most effective ways to assess the reliability of these systems is the evaluation of rainfall forecasting and simulation subsystem in the study basin. The forecasting and simulation subsystem includes meteorological and hydrological models that need to be evaluated for the model's accuracy. In the simulation subsystem of the present study, a meteorological model called WRF was used. To run the model, two events were selected from April 12 and 24 May 2020, which caused human and financial damage to the province. Besides, these events represent the highest rainfall of the year. Then, using statistical calculations, the model was verified. The accuracy of the WRF model is 66% and 63% for the rainfall threshold of ≥ 5 mm of the observation quantity. If the rainfall threshold is ≥ 1 mm, the accuracy of the WRF model reaches 98%. Evaluating the FAR showed that the WRF model in the Lin scheme has the lowest quantity with 36%. The WSM5 scheme has the highest quantity with 75%. This value in the design of different variants is different. The FAR is 25% and 30% for the amount of rainfall, while the alarming ratio for simulation and forecasting of rainfall in all study schemes is below 5%. The result of evaluating the correlation of the test between different schemes of studies showed that for the summer event (24 May), the schemes of the WRF model have a stronger correlation in both cold and temperate mountain climates. Therfore, the value of correlation coefficient between observation data and simulation where about 98% in Lin and, WDM5 schemes .. The results of the WRF scheme for the spring event (12 April) showed that the temperate mountainous climate had a weaker correlation between observation data and simulation data due to temperatures this day. A review of the final results showed the WRF model for flood forecasting and warning in the study area. Since this region has a different climatic diversity, WRF model schemes should be selected according to each of these climates and different seasons. Also, the results of this study showed that Lin schemas are suitable for desert/semi-desert climates, WSM3, WSM5, and WSM6 for temperate mountain/cold mountain climates, and WDM5 for desert and cold mountain climates. Then, according to the accuracy of the simulation results, the selected schemes of the WRF model can be used to forecast rainfall in the next 24 h. Finally, by forecasting rainfall and using the numerical output of this meteorological model in hydrological models, one can be aware of the warnings and dangers of sudden floods in the next 24 h.

Author contribution All the authors contributed to the study's conception and design. Material preparation, data collection, and analysis were performed by Rasoul Sarvestan, Mokhtar Karami, and Reza Javidi Sabaghian. The first draft of the manuscript was written by Rasoul Sarvestan and all the authors commented on previous versions of the manuscript. All the authors read and approved the final manuscript.

Funding This paper is part of the PhD thesis at the Hakim Sabzevari University of Iran. And it has been done with the financial support Regional Water Company of Khorasan Razavi.

Availability of data and material Not applicable.

Code availability Not applicable.

Declarations

Conflict of interest The authors declare that they have no competing interests.

Ethics approval Not applicable.

Consent to participate Not applicable.

Consent for publication All the authors consent to the publication of the article after acceptance.

References

Amorim J da S, Viola, Junqueira, de Oliveira Marcelo RRubens-Vinicius A, de Mello. Carlos R (2020) Evaluation of satellite precipitation products for hydrological modeling in the Brazilian Cerrado Biome. Water 12:2571

Bárdossy A, Das T (2008) Influence of rainfall observation network on model calibration and application. Hydrology and Earth System Sciences Discussions 12:77–89

Basin, Ganga. 2017. Assessment of the Weather Research and Forecasting (WRF) model for extreme rainfall event simulations in the upper. *Hydrol. Earth Syst. Sci.* 1–29.

Bayat B, Hosseini K, Nasseri M, Karami H (2019) Challenge of rainfall network design considering spatial versus spatiotemporal variations. J Hydrol 574:990–1002

Bhimala KR, Gouda KC (2021) 'Evaluating the spatial distribution of WRF-simulated rainfall, 2-m air temperature, and 2-m relative humidity over the urban region of Bangalore, India. Pure Appl Geophys 178:1105–1120

Cao Qimin, Jiang Baolin, Shen Xiaodian, Lin Wenshi, Chen Junwen (2021) Microphysics effects of anthropogenic aerosols on urban heavy precipitation over the Pearl River Delta. China. Atmospheric Research 253:105478

Casagli N, Dapporto S, Ibsen ML, Tofani V, Vannocci P (2006) "Analysis of the landslide triggering mechanism during the storm of 20th–21st November 2000 Northern Tuscany." Landslides 3:13–21

Chawla I, Osuri KK, Mujumdar PP, Niyogi D (2018) Assessment of the Weather Research and Forecasting (WRF) model for simulation of extreme rainfall events in the upper Ganga Basin. Hydrol Earth Syst Sci 22:1095–1117

Chen X, Hossain F (2018) Understanding model-based probable maximum precipitation estimation as a function of location and season from atmospheric reanalysis. J Hydrometeorol 19:459–475

Cong X-y, Ni G-H, Hui S-b, Tian F-Q, Zhang T (2006) Simulative analysis on storm flood in typical urban region of Beijing based on SWMM. Water Resources and Hydropower Engineering 4:64–67

Evans, James E, Scudder D Mackey, Johan F Gottgens, and Wilfrid M Gill. 2000. 'Lessons from a dam failure'.

Gadgil S, Sajani S (1998) Monsoon precipitation in the AMIP runs. Clim Dyn 14:659–689

Garambois PA, Roux H, Larnier K, Labat D, Dartus D (2015) Characterization of catchment behaviour and rainfall selection for flash flood hydrological model calibration: catchments of the eastern Pyrenees. Hydrol Sci J 60:424–447

Gerber F, Besic N, Sharma V, Mott R, Daniels M, Gabella M, Berne A, Germann U, Lehning M (2018) Spatial variability in snow precipitation and accumulation in COSMO–WRF simulations and radar estimations over complex terrain. Cryosphere 12:3137–3160

Ghazali DA, Guericolas M, Thys F, Sarasin F, Gonzalez PA, Casalino E (2018) Climate change impacts on disaster and emergency medicine focusing on mitigation disruptive effects: an international perspective. Int J Environ Res Public Health 15:1379

Goodarzi L, Banihabib ME, Ghafarian P, Roozbahani A (2018) Evaluation and comparison of global ensemble prediction systems for probabilistic forecasting of heavy rainfalls (case study: Kan Basin, Iran). Physical Geography Research Quarterly 50:195–205

Guo J, Lei H, Chen Di, Yang J (2019) Evaluation of the WDM6 scheme in the simulation of number concentrations and drop size distributions of warm-rain hydrometeors: comparisons with the observations and other schemes. Atmospheric and Oceanic Science Letters 12:458–466

Hadilooie, Hassan, Majid Azadi, Mohammad Memarian, and M Mohammad. 2014. 'Evaluating the performance of WRF cloud microphisycal schemes', *Thesis Submitted For the Degree of M. Sc. in Meteorology*: 1- 92.

Hong S-Y, Dudhia J, Chen S-H (2004) A revised approach to ice microphysical processes for the bulk parameterization of clouds and precipitation. Mon Weather Rev 132:103–120

Hong S-Y, Lim J-O (2006) The WRF single-moment 6-class microphysics scheme (WSM6). Asia-Pac J Atmos Sci 42:129–151

Hong, Song-You, Kyo-Sun Sunny Lim, Yong-Hee Lee, Jong-Chul Ha, Hyung-Woo Kim, Sook-Jeong Ham, and Jimy Dudhia. 2010. 'Evaluation of the WRF double-moment 6-class microphysics scheme for precipitating convection', *Advances in Meteorology*, 2010.

Hsiao L-F, Yang M-J, Lee C-S, Kuo H-C, Shih D-S, Tsai C-C, Wang C-J, Chang L-Y, Chen D-C, Feng L (2013) Ensemble forecasting of typhoon rainfall and floods over a mountainous watershed in Taiwan. J Hydrol 506:55–68

https://www.mmm.ucar.edu/weather-research-and-forecasting-model.

Hu C, Liu C, Yao Y, Qiang Wu, Ma B, Jian S (2020a) Evaluation of the impact of rainfall inputs on urban rainfall models: a systematic review. Water 12:2484

Hu, Lanxin, Efthymios I Nikolopoulos, Francesco Marra, Efrat Morin, Marco Marani, and Emmanouil N Anagnostou. 2020. 'Evaluation of MEVD-based precipitation frequency analyses from quasi-global precipitation datasets against dense rain gauge networks', *Journal of Hydrology*, 590: 125564.

Iran meteorological office. 2019. "Precipitation, temperature and evapotranspiration data in the Khorasan Razavi province." In. Irain: Meteorological Office of Iran.

Kakolaki, R, M Memarian, N Esfahany, and nori.T. 2016. 'Study of the mechanism of summer precipitetions occurrence in the southern of iran using the WRF model (Case Study)', *Yazd University*: 1–117.

Kamyabi S (2016) Implementing climate classification system architecture in Khorasan Razavi. Geographical Territory 13:91–105

Kidd C, Becker A, Huffman GJ, Muller CL, Joe P, Skofronick-Jackson G, Kirschbaum DB (2017) So, how much of the Earth's surface is covered by rain gauges? Bull Am Meteor Soc 98:69–78

Kitanidis PK, Bras RL (1980) 'Real-time forecasting with a conceptual hydrologic model: 1. Anal Uncertainty Water Resour Res 16:1025–1033

Kodamana R, Fletcher CG (2021) Validation of CloudSat-CPR derived precipitation occurrence and phase estimates across Canada. Atmosphere 12:295

Kusaka H, Crook A, Dudhia J, Wada K (2005) Comparison of the WRF and MM5 models for simulation of heavy rainfall along the Baiu front. Sola 1:197–200

Langkamp T, Böhner J (2011) Influence of the compiler on multi-CPU performance of WRFv3. Geoscientific Model Development 4:611–623

Li, Pin-Lun, Chia-Jeng Chen, and Liao-Fan Lin. 2021. 'Hydrometeorological assessment of satellite and model precipitation products over Taiwan', *Journal of Hydrometeorology*.

Liu J, Bray M, Han D (2012) Sensitivity of the Weather Research and Forecasting (WRF) model to downscaling ratios and storm types in rainfall simulation. Hydrol Process 26:3012–3031

Liu J, Wang J, Pan S, Tang K, Li C, Han D (2015) A real-time flood forecasting system with dual updating of the NWP rainfall and the river flow. Nat Hazards 77:1161–1182

Mahala BK, Mohanty PK, Xalxo KL, Routray A, Misra SK (2021) Impact of WRF parameterization schemes on track and intensity of extremely severe cyclonic storm "Fani." Pure Appl Geophys 178:245–268

McClymont K, Morrison D, Beevers L, Carmen E (2020) Flood resilience: a systematic review. J Environ Planning Manage 63:1151–1176

Minamiguchi Y, Shimadera H, Matsuo T, Kondo A (2018) Numerical simulation of heavy rainfall in August 2014 over Japan and analysis of its sensitivity to sea surface temperature. Atmosphere 9:84

Mohammadiha, Amir, Mohammad Memarian, Majid Azadi, and Reyhani Parvari. 2012. 'Verification of WRF model forecatings for content of precipitable water and precipitation with the RADAR data', *Thesis submitted For the degree of M.Sc*: 1–160.

Naing, Su Myat. 2021. 'Sensitivity analysis of heavy rainfall events on physical parameterization configurations using WRF-ARW model over Myanmar'.

Papathanasiou C, Makropoulos C, Mimikou M, and, (2015) Hydrological modelling for flood forecasting: calibrating the post-fire initial conditions. J Hydrol 529:1838–1850

Que L-J, Que W-L, Feng J-M (2016) Intercomparison of different physics schemes in the WRF model over the Asian summer monsoon region. Atmospheric and Oceanic Science Letters 9:169–177

Ratna SB, Sikka DR, Dalvi M, Venkata J, Ratnam. (2011) Dynamical simulation of Indian summer monsoon circulation, rainfall and its interannual variability using a high resolution atmospheric general circulation model. Int J Climatol 31:1927–1942

Ridwan, Wanie M, Michelle Sapitang, Awatif Aziz, Khairul Faizal Kushiar, Ali Najah Ahmed, and Ahmed El-Shafie. 2020. 'Rainfall forecasting model using machine learning methods: case study Terengganu, Malaysia', *Ain Shams Engineering Journal*.

Shahrban, Mahshid, Jeff Walker, Q Wang, Alan Seed, Peter Steinle, F Chan, D Marinova, and R Anderssen. 2011. "Comparison of weather radar, numerical weather prediction and gauge-based rainfall estimates." In *Proc. 19th International Congress on Modelling and Simulation, Perth*, 3384–90.

Skamarock, WC, JB Klemp, J Dudhia, DO Gill, DM Barker, MG Duda, XYW Huang, and JG Wang Powers. 2008. 'A description of the advanced research WRF Version 3, 125pp', *NCAR Tech. Note NCAR/TN-475+ STR*.

Skamarock, William C, JB Klemp, J Dudhia, DO Gill, DM Barker, W Wang, and JG Powers. 2005. "A description of the Advanced Research WRF version 2. NCAR Tech." In.: Note NCAR/TN-4681STR.

Srinivas CV, Hariprasad D, Bhaskar Rao DV, Anjaneyulu Y, Baskaran R, Venkatraman B (2013) Simulation of the Indian summer monsoon regional climate using advanced research WRF model. Int J Climatol 33:1195–1210

Statistical yearbook, Khorasan Razavi province. 2019. 'Land and climate', *Statistics Center of Iran*: 115–25.

Steduto P, Hsiao TC, Raes D, Fereres E (2009) 'AquaCrop—the FAO crop model to simulate yield response to water: I. Concepts and Underlying Principles. Agron J 101:426–437

Tahir, Wardah, Ahmad Kamil Aminuddin, Suzana Ramli, and Jurina Jaafar. 2017. 'Quantitative precipitation forecast using numerical weather prediction and meteorological satellite for Kelantan and Klang river basins', *Jurnal Teknologi*, 79.

Tian J, Liu J, Wang J, Li C, Fuliang Yu, Chu Z (2017) A spatio-temporal evaluation of the WRF physical parameterisations for numerical rainfall simulation in semi-humid and semi-arid catchments of Northern China. Atmos Res 191:141–155

Tian J, Liu J, Yan D, Ding L, Li C (2019) Ensemble flood forecasting based on a coupled atmospheric-hydrological modeling system with data assimilation. Atmos Res 224:127–137

Wang, Jun, Bormin Huang, Allen Huang, and Mitchell D Goldberg. 2011. "Parallel computation of the weather research and forecast (wrf) wdm5 cloud microphysics on a many-core gpu." In *2011 IEEE 17th International Conference on Parallel and Distributed Systems*, 1032–37. IEEE.

Wong DC, Pleim J, Mathur R, Binkowski F, Otte T, Gilliam R, Pouliot G, Xiu A, Young JO, Kang D (2012) WRF-CMAQ two-way coupled system with aerosol feedback: software development and preliminary results. Geoscientific Model Development 5:299–312

Xavier AC, King CW, Scanlon BR, and, (2016) Daily gridded meteorological variables in Brazil (1980–2013). Int J Climatol 36:2644–2659

Yang T-H, Yang S-C, Ho J-Y, Lin G-F, Hwang G-D, Lee C-S (2015) Flash flood warnings using the ensemble precipitation forecasting technique: a case study on forecasting floods in Taiwan caused by typhoons. J Hydrol 520:367–378

Yatheendradas, Soni, Thorsten Wagener, Hoshin Gupta, Carl Unkrich, David Goodrich, Mike Schaffner, and Anne Stewart. 2008. 'Understanding uncertainty in distributed flash flood forecasting for semiarid regions', *Water Resources Research*, 44.

Yonese, Yoshitomo, Akira Kawamura, Hideo Amaguchi, and 2018. "Storm runoff prediction using rainfall radar map supported by global optimization methodology." In *Ibero-American Conference on Artificial Intelligence*, 507–17. Springer.

Zhang L, Gong S, Zhao T, Zhou C, Wang Y, Li J, Ji D, He J, Liu H, Gui Ke (2021) Development of WRF/CUACE v1. 0 model and its preliminary application in simulating air quality in China. Geoscientific Model Development 14:703–718

Zhu Jingxuan, Zhang Shuliang, Yang Qiqi, Qi Shen Lu, Zhuo, and Qiang Dai. (2021) Comparison of rainfall microphysics characteristics derived by numerical weather prediction modelling and dual-frequency precipitation radar. Meteorological Applications 28:e2000